THE JOURNAL OF PHYSICAL CHEMISTRY C

Article

pubs.acs.org/JPCC

Facile Synthesis of an Extensive Family of $Sc_2O@C_{2n}$ (n = 35−47) and Chemical Insight into the Smallest Member of $Sc_2O@C_2(7892)-C_{70}$

Meirong Zhang,[†,⊥] Yajuan Hao,[†] Xiaohong Li,[‡] Lai Feng,*[,†] Ting Yang,[‡] Yingbo Wan,[‡] Ning Chen,*[,‡] Zdeněk Slanina,*[,§] Filip Uhlík,[∥] and Hailin Cong*[,⊥]

[†]College of Physics, Optoelectronics and Energy & Collaborative Innovation Center of Suzhou Nano Science and Technology, Soochow University, Suzhou 215006, China

[‡]College of Chemistry, Chemical Engineering and Materials Science, Soochow University, Suzhou 215163, China

[§]Life Science Center of Tsukuba Advanced Research Alliance, University of Tsukuba, Tsukuba 305-8577, Japan

[∥]Department of Physical and Macromolecular Chemistry, Faculty of Science, Charles University in Prague, Albertov 6, 128 43 Praha 2, Czech Republic

[⊥]Lab for New Fiber Materials and Modern Textile-Growing Base for State Key Laboratory, College of Chemical and Environmental Engineering, Qingdao University, Qingdao 266071, China

Supporting Information

ABSTRACT: An extensive family of oxide cluster fullerenes (OCFs) $Sc_2O@C_{2n}$ (n = 35−47) has been facilely produced for the first time by introducing CO_2 as the oxygen source. Among this family, $Sc_2O@C_{70}$ was identified as the smallest OCF and therefore isolated and characterized by mass spectrometry, ^{45}Sc nuclear magnetic resonance, UV−vis−near-infrared absorption spectroscopy, cyclic voltammetry, and density functional theory calculations. The combined experimental and computational studies reveal a non-isolated pentagon rule isomer $Sc_2O@C_2(7892)-C_{70}$ with reversible oxidative behavior and lower bandgap relative to that of $Sc_2S@C_2(7892)-C_{70}$, demonstrating a typical example of unexplored OCF and underlining its cluster-dependent electronic properties.

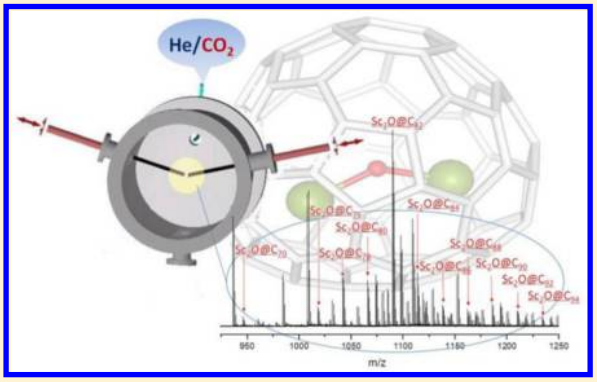

1. INTRODUCTION

Since the discovery of fullerenes, their three-dimensional structures and unique properties have attracted great interests.[1,2] In particular, inside fullerene cage there is a nanometer-sized space that is big enough to accommodate a cluster of heteroatoms or even a small molecule. On the basis of this knowledge, in the past decade, many efforts have been devoted to the science of endohedral fullerenes.[3−9] It has been well demonstrated that a variety of metal, nonmetal atoms, or even small molecules can be encapsulated into a fullerene cage using physical or chemical methods, resulting in stable endohedrals such as $H_2@C_{60}$,[10,11] $N@C_{60}$,[12−14] $Gd_3N@C_{2n}$,[15] and $H_2O@C_{60}$.[16] These endohedrals are potentially useful in the fields of molecular electronics, hydrogen storage, and medical and material sciences.[17−23]

Particularly, it has been approved that most group 2−3 elements and lanthanides can be trapped inside a fullerene cage in the form of M_x (x = 1−3),[24−27] or a cluster of metal carbide M_xC_2 (x = 2−4),[28−32] metal nitride M_3N,[33−35] metal sulfide M_2S,[36−38] metal cyanide M_xNC (x = 1,3),[39−41] or even metal oxide $Sc_2O/Sc_4O_2/Sc_4O_3$,[42−44] giving rise to the formation of endohedral metallofullerenes (EMFs). For bulk preparations of EMFs, the Krätschmer−Huffman generator has been widely used since 1991,[45] in which a graphite anode containing metal oxide or metallic alloy is evaporated in an electric arc under a low-pressure helium atmosphere. Noteworthy is that, as for the production of nitride, cyanide, or sulfide cluster fullerenes, additional nitrogen and sulfur sources are very essential, which may be provided by either reactive gases (i.e., N_2,[33] NH_3,[46] or SO_2[37]) or solid compounds containing nitrogen or sulfur element (i.e., guanidium thiocyanate[36]). As demonstrated by previous experiments, the gaseous additives usually give rise to better productions than the solid additives probably due to their significant stabilities and homogeneities

Compared to those well-studied cluster fullerenes, oxide cluster fullerenes (OCFs) are relatively less-explored. Up to now, only a few OCFs including $Sc_4O_{2-3}@C_{80}$ and $Sc_2O@C_{82}$ have been reported.[42] According to the authors, the introduction of a small amount of air might provide the oxygen source for the OCF synthesis. However, such method resulted in, besides empty fullerenes, mainly nitride cluster fullerenes along with limited varieties of OCFs.[43] Herein, we

Received: October 2, 2014
Revised: November 17, 2014
Published: November 19, 2014

   dx.doi.org/10.1021/jp509975w | J. Phys. Chem. C 2014, 118, 28883−28889

demonstrate that an extensive family of scandium OCFs with cage size ranging from C_{70} to C_{94} can be synthesized in macroscopic quantities by introducing CO_2 as the oxygen source. In addition, $Sc_2O@C_{70}$, the smallest OCF identified by means of mass spectroscopy, has been isolated and characterized for the first time.

2. EXPERIMENTAL SECTION

2.1. Synthesis and Isolation. A new family of scandium OCFs $Sc_2O@C_{2n}$ was synthesized in a typical Krätschmer–Huffman arc reactor. The details are briefly described as follows. The graphite anode was filled with a mixture of Sc_2O_3 and graphite powder with a molar ratio of 1:1 and was annealed at 1000 °C for 10 h under Ar atomosphere before use. The DC-arc discharging was carried out under 3×10^4 pa He/CO_2 atmosphere (the ratio of He/CO_2 is 9/1 in volume) and current of 100 A. After DC-arc discharging, the generated soot was collected under ambient conditions, and the mixture was Soxhlet extracted by chlorobenzene for 18 h. The resulting dark brown solution was evaporated to remove chlorobenzene, immediately redissolved in toluene, and subsequently passed through a 0.45 μm Telflon filter for HPLC separation. The separation of $Sc_2O@C_{2n}$ was performed by a multistep HPLC procedure using columns including Buckyprep M column (25 mm × 250 mm, Nacalai Tesque, Japan), Buckyprep column (10 mm × 250 mm, Nacalai Tesque, Japan), and 5PBB column (10 mm × 250 mm, Nacalai Tesque, Japan).

The mass characterization was done by matrix-assisted laser desorption/ionization time-of-flight (MALDI-TOF) mass spectrometry using the Biflex III spectrometer (Bruker, Germany) with positive- and negative-ion modes, respectively. UV–vis–near-infrared (NIR) spectrum of the purified OCF sample was measured in toluene solution with an UV 3600 spectrometer (Shimadzu, Japan) using a quartz cell of 1 mm layer thickness and 1 nm resolution. The ^{45}Sc nuclear magnetic resonance (NMR) spectroscopic study was performed at 145 MHz with a Agilent 600 MHz NMR spectrometer at 25 °C in CS_2 solution with D_2O as the lock and a 0.4 M $Sc(NO_3)_3$ solution in D_2O as the reference.

Cyclic voltammetry (CV) and differential pulse voltammetry (DPV) were carried out in *o*-dichlorobenzene (*o*-DCB) using a CHI-660E instrument. A conventional three-electrode cell consisting of a platinum working electrode, a platinum counter-electrode, and a saturated calomel reference electrode (SCE) was used for both measurements. $(n\text{-}Bu)_4NPF_6$ (0.05 M) was used as the supporting electrolyte. All potentials were recorded against a SCE reference electrode and corrected against Fc/Fc^+. CV and DPV were measured at a scan rate of 100 and 20 mV s^{-1}, respectively.

2.2. Computational Method. All calculations were carried out using the Gaussian 09 program package. Geometry optimizations and population analysis were performed using the density functional theory with the recently introduced M06-2X functional, 3-21G basis set for the C and O atoms, and the SDD basis set (with the SDD effective core potential) for Sc atom (the M06-2X/3-21G~SDD level). The orbital energies and distributions were calculated at a higher level (the M06-2X/6-311G*~SDD level). Time dependant (TD) DFT calculations were performed at the B3LYP/6-311G~*SDD level.

3. RESULTS AND DISCUSSION

A series of scandium OCFs $Sc_2O@C_{2n}$ (n = 35–47) were synthesized in a typical Krätschmer–Huffman arc reactor under a He/CO_2 atmosphere. The as-prepared soot was Soxhlet extracted with chlorobenzene. As shown in Figure 1, which

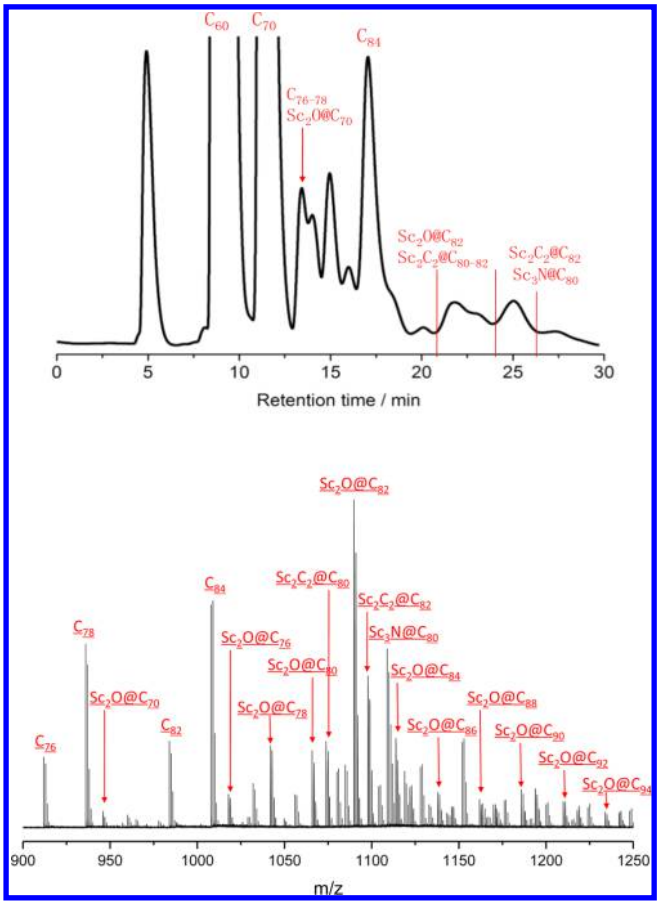

Figure 1. HPLC profile of the extracted fullerene mixture containing the OCF family (up); MALDI-TOF mass spectrum of the HPLC fraction with retention time longer than 13 min (down), showing the presence of OCF family $Sc_2O@C_{2n}$ (n = 35–47).

demonstrates the high-performance liquid chromatography (HPLC) profile of the extracted fullerene mixture, the empty fullerenes C_{60} and C_{70} are seen as the major products and eluted before 13 min on a Buckprep-M column. The fractions with retention time longer than 13 min were collected and analyzed by mass spectroscopy. As shown in Figure 1, a series of scandium OCFs $Sc_2O@C_{2n}$ with cage size ranging from C_{70} to C_{94} can be identified in the mass spectrum, most of which have never been reported before. Besides, typical nitride cluster fullerenes and carbide cluster fullerenes, for example, $Sc_3N@C_{80}$ and $Sc_2C_2@C_{82}$, are also detectable in the mass spectrum. Nevertheless, their contents are found to be lower than that of the most abundantly yielded OCF $Sc_2O@C_{82}$ according to a combined analysis of HPLC and mass spectrum, indicating a selective synthesis of OCFs under our employed conditions. In contrast, in a control experiment, where a He/air atmosphere was utilized, besides empty fullerenes, mainly nitride cluster fullerenes were obtained, while only a trace of $Sc_2O@C_{82}$ was detected (see Figure S1, Supporting Information), which agrees well with the previous report.[43] Thus, this comparative study suggests that CO_2 is a better oxygen source than air for the

dx.doi.org/10.1021/jp509975w | J. Phys. Chem. C 2014, 118, 28883–28889

production of OCFs. Moreover, in another control experiment, where pure He atmosphere was employed, the most abundantly produced metallofullerene was found to be $Sc_2C_2@C_{82}$ rather than $Sc_2O@C_{82}$ (see Figure S2, Supporting Information). It appears that the introduction of CO_2 causes a significant increase of the relative yields of OCFs and suppresses the generation of carbide cluster fullerenes, which are otherwise abundantly yielded under pure helium atmosphere.

As the mass spectrum (Figure 1) shows, in this OCF family, the smallest fullerene that can be identified by far is $Sc_2O@C_{70}$. A combined analysis of HPLC and mass spectroscopy suggests that the $Sc_2O@C_{70}$ fraction overlaps with those of C_{76} and C_{78} and is eluted with a retention time of around 15 min on a Buckyprep-M column (see Figure S3, Supporting Information). $Sc_2O@C_{70}$ was further separated using a Buckyprep column and a 5PBB column, which resulted in the isolation of a pure sample of $Sc_2O@C_{70}$ (see Figures S4−5, Supporting Information). Compared to other OCFs, the yield of $Sc_2O@C_{70}$ is relatively lower. By consuming 90 packed graphite rods, only ca. 2 mg of $Sc_2O@C_{70}$ was obtained after HPLC purification.

The composition of $Sc_2O@C_{70}$ was confirmed by MALDI-TOF mass spectroscopy. As shown in Figure 2, the purified

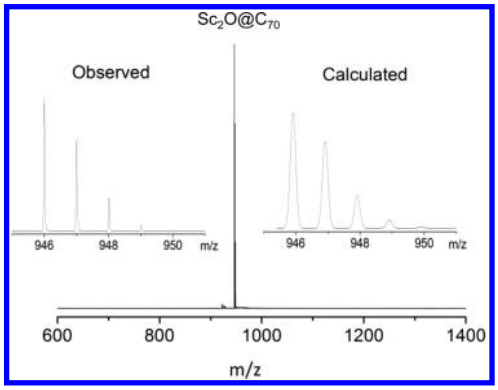

Figure 2. MALDI-TOF mass spectrum of the purified sample $Sc_2O@C_{70}$ in a positive-ion reflection mode. The insets show the observed and calculated isotopic distributions of $Sc_2O@C_{70}$.

sample of $Sc_2O@C_{70}$ shows a predominant signal at 946 m/z, and its observed isotopic distribution agrees very well with the calculated values. Moreover, the ^{45}Sc NMR spectrum of $Sc_2O@C_{70}$ was measured at room temperature. As shown in Figure 2, a ^{45}Sc NMR signal at 32.4 ppm is clearly seen, suggesting that the two Sc ions are either equivalent or undergo fast rotation inside the cage. However, because of the small amount of the sample, the ^{13}C NMR data is not available.

The purified sample of $Sc_2O@C_{70}$ shows a brown color in toluene solution and its UV−vis−NIR spectrum exhibits (see Figure 3) a broad and strong absorption centered around 1188 nm along with other relatively weaker absorptions at 393, 459, 497, 706, and 1015 nm. Such absorption feature is different from that of previously reported $Sc_3N@C_{2v}(7854)-C_{70}$[47] but is very similar to that of $Sc_2S@C_2(7892)-C_{70}$,[48] which displays a broad absorption around 1102 nm along with a few weak absorptions in other spectral regions. Because the absorptions of fullerenes in the visible and NIR region are dominated by the $\pi-\pi^*$ transitions of the carbon cages and the spectra are very sensitive to the cage symmetry,[49] such spectral similarities between $Sc_2O@C_{70}$ and $Sc_2S@C_{70}$ might suggest their same cage symmetry as well as the similar electronic structure.

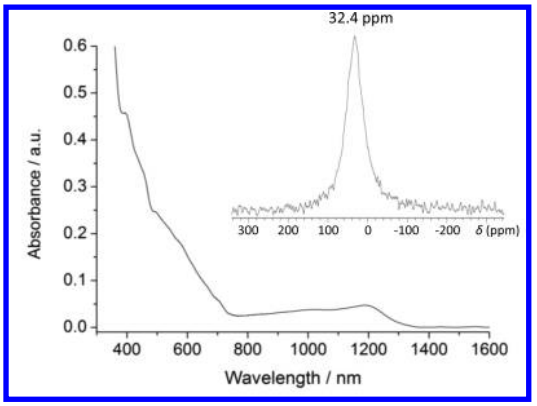

Figure 3. UV−vis−NIR absorption spectrum of $Sc_2O@C_{70}$ in toluene solution. Inset shows the ^{45}Sc NMR spectrum of $Sc_2O@C_{70}$, measured in CS_2 with D_2O as the lock and a 0.4 M $Sc(NO_3)_3$ solution in D_2O as the reference.

Nevertheless, note that not only the first absorption but also the onset position of $Sc_2O@C_{70}$ (i.e., 1325 nm) is red-shifted by ca. 80−100 nm with respect to those of $Sc_2S@C_{70}$, indicating a smaller band gap of $Sc_2O@C_{70}$ relative to that of $Sc_2S@C_{70}$.

To further shed light onto the structural and electronic features of $Sc_2O@C_{70}$, a series of computational studies were performed to assign the cage symmetry among 8149 possible isomers. In fact, we studied only four $Sc_2O@C_{70}$ isomers, namely, $Sc_2O@D_{5h}(8149)-C_{70}$, $Sc_2O@C_2(7892)-C_{70}$, $Sc_2O@C_2(7957)-C_{70}$, and $Sc_2O@C_1(7924)-C_{70}$, based on the following considerations: (i) The density functional theory (DFT) based population analysis on the optimized $Sc_2O@C_{70}$ isomers reveals that there is a formal transfer of four electrons between the cluster and the cage, and the electronic structure can be described as $(Sc_2O)^{4+}@(C_{70})^{4-}$. (ii) A tetraanionic cluster may possibly fit well in a cage satisfying isolated pentagon rule (IPR) or a non-IPR cage with two or less adjacent pentagon pairs (APPs).[8] (iii) According to the previous work, the tetraanions of these IPR or non-IPR C_{70} cages show lower relative energies with respect to the others.[48] Therefore, our computations involving only the OCFs corresponding to the lowest-energy tetraanionic cages shall be reasonable and more extensive computations are not very necessary. The relative energies of these optimized isomeric $Sc_2O@C_{70}$ structures are listed in Table 1. Among them, $Sc_2O@C_2(7892)-C_{70}$ is found to be the lowest-energy isomer at the M06-2X/3-21G~SDD level of theory,[50−52] at least 20 kcal mol^{-1} lower than the others, despite the fact that the tetraanion of the empty IPR cage $D_{5h}(8149)-C_{70}$ exhibits the lowest energy. This situation is very similar to the case of $Sc_2S@C_{70}$, in which $Sc_2S@C_2(7892)-C_{70}$ is 18 kcal mol^{-1} more stable than others at the BP86/TZP level.[48] Thus, it appears that the encapsulation of either a Sc_2O cluster or a Sc_2S cluster, which are valence isoelectronic (i.e., $(Sc_2X)^{4+}$, X = O or S), renders the non-IPR cage of $C_2(7892)-C_{70}$ higher stability with respect to the other isomers.

In particular, the Sc−O−Sc angle in the optimized $Sc_2O@C_2(7892)-C_{70}$ was identified as 139.23°, much larger than that for $Sc_2S@C_2(7892)-C_{70}$ (98.96°), which was optimized at the same computational level (see Figure 4). Despite the uncertainty of the DFT-optimized structures, noteworthy is that such a Sc−X−Sc (X = S or O) angle difference ($\Delta\theta \approx 40°$) is very comparable to that found between $Sc_2S@C_s(6)-C_{82}$ and

dx.doi.org/10.1021/jp509975w | J. Phys. Chem. C 2014, 118, 28883−28889

Table 1. Relative Energies (in kcal mol^{-1}) for Four C_{70} Isomers in the Tetraanion and Endohedral Forms

	C_{70}–D_{5h} (IPR;8149)	C_{70}–C_2(7892)	C_{70}–C_2(7957)	C_{70}–C_1(7924)
$(C_{70})^{4-a}$	0.0	3.9	4.7	11.6
$Sc_2S@C_{70}$[a]	20.6	0.0	19.1	18.6
$Sc_2O@C_{70}$[b]	35.06	0.0	33.50	23.11

[a]Data in ref 48. [b]Data calculated at the M06-2X/3-21G~SDD level.

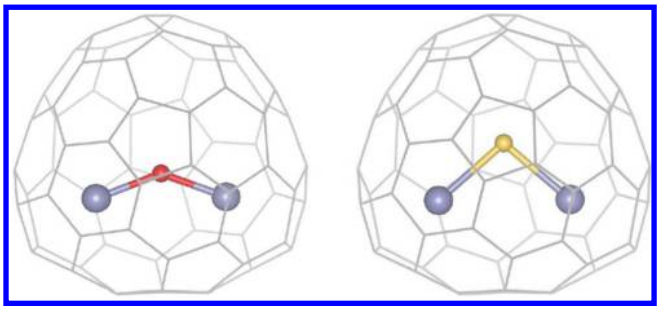

Figure 4. DFT-optimized $Sc_2O@C_2(7892)$–C_{70} (left) and $Sc_2S@C_2(7892)$–C_{70} (right) at the M06-2X/3-21G~SDD level.

$Sc_2O@C_s(6)$–C_{82}, which have a Sc–S–Sc angle of 113.8° and a Sc–O–Sc angle of 156.6°, respectively, according to the X-ray analysis.[38,43] It appears that in the small or middle-sized fullerene cage the Sc_2O cluster is more linearly aligned, as compared to the Sc_2S cluster, probably due to the shorter Sc–O distance (i.e., 1.896 Å for $Sc_2O@C_2(7892)$–C_{70}) with respect to the Sc–S distance (i.e., 2.365 Å for $Sc_2O@C_2(7892)$–C_{70}). Moreover, the Mulliken atomic charges on Sc and O in the Sc_2O cluster are calculated to be +2.082 e and −0.539 e, respectively, while the values for Sc_2S cluster are +1.805 e for Sc and +0.026 e for S. Such Mulliken charge difference can be explained by the higher electronegativity of O relative to that of S (i.e., 3.610 for O and 2.589 for S)[53] and suggests different electronic configuration of these encaged clusters. Nevertheless, in the optimized $Sc_2O@C_2(7892)$–C_{70}, each scandium ion of the cluster is equally approaching a pentalene motif, which resembles that of $Sc_2S@C_2(7892)$–C_{70}, suggesting their similar cluster-cage interactions. Such a cluster-cage contact has also been found in most cluster fullerenes with non-IPR cages, for example, $Sc_3N@D_3(6140)$–C_{68},[54] $Gd_3N@C_s(39663)$–C_{82},[55] and $Sc_2S@C_s(10528)$–C_{72},[56] which results in localized electron transfer between the cluster and the pentalene motif. Therefore, despite some geometric and electronic differences, Sc_2O and Sc_2S clusters apparently play similar roles on the selection of cage isomer, along with the electronic stabilization resulting from the similar cluster–cage interactions.

The orbital energy levels as well as the orbital distributions of $Sc_2O@C_2(7892)$–C_{70} have been further calculated at the M06-2X/6-311G*~SDD level. As shown in Figure 5, both the HOMO and LUMO are mainly contributed by the cage orbitals with small but salient contributions from the metal cluster. Substantial orbital overlap between the cage and cluster can be clearly identified, indicating both the covalent and ionic interactions between the cluster and fullerene cage. Thus, the computation results suggest two equivalent Sc ions in a rotationally hindered Sc_2O cluster for $Sc_2O@C_2(7892)$–C_{70}, which agrees well with the experimentally observed single ^{45}Sc NMR signal. However, the HOMO energy level of $Sc_2O@C_2(7892)$–C_{70} is calculated as −6.07 eV at the M06-2X/6-311G*~SDD level, 0.07 eV higher than that of $Sc_2S@C_2(7892)$–C_{70} (i.e., −6.14 eV calculated at the same level), while the LUMO is −2.99 eV, 0.07 eV lower than that of $Sc_2S@C_2(7892)$–C_{70} (i.e., −2.92 eV calculated at the same level). Thus, the bandgap of $Sc_2O@C_2(7892)$–C_{70} is determined as 3.08 eV, 0.14 eV smaller than that of $Sc_2S@C_2(7892)$–C_{70} (i.e., 3.22 eV). These results agree very well with their spectral comparison, which indicates a smaller bandgap of $Sc_2O@C_2(7892)$–C_{70} compared to that of $Sc_2S@C_2(7892)$–C_{70}. It appears that, despite the identical cage symmetry as well as the similar cluster–cage interactions, slightly varying the endohedral composition from Sc_2S to Sc_2O indeed gives rise to a fine modulation on the MO energy levels as well as on the bandgaps of cluster fullerenes.

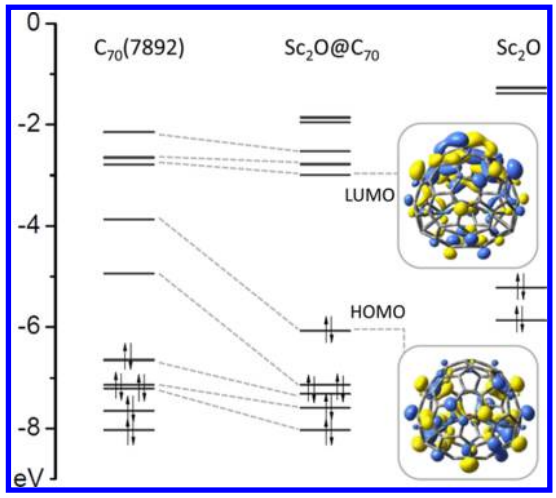

Figure 5. Molecular orbital diagram for $Sc_2O@C_2(7892)$–C_{70}. The fragments, Sc_2O and $C_2(7892)$–C_{70}, were calculated with the geometry that they have in the endohedral fullerene.

The electronic spectra of $Sc_2O@C_2(7892)$–C_{70} and $Sc_2S@C_2(7892)$–C_{70} were also computed using time-dependent (TD)-DFT at the B3LYP/6-311G*~SDD level. Their most intense lowest-energy excitations are listed in Table 2. Particularly, the lowest excitation energy of $Sc_2O@C_2(7892)$–C_{70} (corresponding to the HOMO–LUMO transition) is calculated as 1.237 eV or a λ of 1002 nm, while a λ of 920 nm is calculated for $Sc_2S@C_2(7892)$–C_{70}. Compared to the experimental values (i.e., 1188 nm for $Sc_2O@C_2(7892)$–C_{70} and 1102 nm for $Sc_2S@C_2(7892)$–C_{70}), all the computed excitation energies are apparently overestimated to a similar extent at our computational level. Nevertheless, the computed energy difference (i.e., 0.11 eV) between the singlet-excited $Sc_2O@C_2(7892)$–C_{70} and $Sc_2S@C_2(7892)$–C_{70} can compare reasonably well with the experimentally estimated difference (i.e., 0.08 eV). These results further underline the influence of internal clusters Sc_2X (X = O or S) on the MO levels of cluster fullerenes and suggest that the $Sc_2O@C_{70}$ and the previously reported $Sc_2S@C_{70}$ share the same cage of $C_2(7892)$–C_{70}.

The electrochemical properties of $Sc_2O@C_{70}$ were studied by means of cyclic voltammogram (CV) and differential pulse

dx.doi.org/10.1021/jp509975w | J. Phys. Chem. C 2014, 118, 28883–28889

Table 2. TD-DFT Calculations for the Most Intense Lowest-Energy Excitations in the Absorption Spectra of $Sc_2O@C_2(7892)-C_{70}$ and $Sc_2S@C_2(7892)-C_{70}$

$Sc_2O@C_2(7892)-C_{70}$				$Sc_2S@C_2(7892)-C_{70}$			
E (eV)	λ (nm)	f^a	leading configurations	E (eV)	λ (nm)	f^a	leading configurations
1.2371	1002.20	0.0120	HOMO → LUMO	1.3476	920.03	0.0131	HOMO → LUMO
1.4018	884.49	0.0063	HOMO → LUMO + 1	1.5310	809.82	0.0057	HOMO → LUMO + 1
1.9866	624.09	0.0086	HOMO → LUMO + 3	2.0102	616.77	0.0085	HOMO → LUMO + 3
2.1191	585.05	0.0101	HOMO − 1 → LUMO	2.2256	557.08	0.0129	HOMO − 1 → LUMO

[a]TD B3LYP/6-311G*~SDD calculations; only excitations with f (oscillator strength) > 0.001 are listed.

voltammogram (DPV), as shown in Figure 6. CV and DPV were recorded in *o*-dichlorobenzene (*o*-DCB) and tetra-(*n*-butyl)-ammonium hexafluoro-phosphate (*n*-Bu_4NPF_6; 0.05 M) was used as supporting electrolyte. All the obtained redox potentials as well as the previously reported redox data of $Sc_2S@C_2(7892)-C_{70}$ are summarized in Table 3. Particularly, in the anodic range, $Sc_2O@C_2(7892)-C_{70}$ shows two reversible oxidation steps with half-waves potentials of 0.10 and 0.55 V, respectively. Such an oxidative behavior is different from that of $Sc_2S@C_2(7892)-C_{70}$, which exhibits a reversible first oxidation at 0.14 V and an irreversible second oxidation at 0.65 V. However, in the cathodic range, the reductive behavior of $Sc_2O@C_2(7892)-C_{70}$ is very similar to that of $Sc_2S@C_2(7892)-C_{70}$,[47] displaying irreversible reductive processes. As DPV shows, three one-electron reductions of $Sc_2O@C_2(7892)-C_{70}$ can be identified at −1.25, −1.66, and −2.15 V, respectively. The electrochemical potential gap of $Sc_2O@C_2(7892)-C_{70}$ is determined as 1.46 and 1.35 V according to the CV and DPV, respectively. Such values are lower than that of $Sc_2S@C_2(7892)-C_{70}$, indicating a smaller band gap of $Sc_2O@C_2(7892)-C_{70}$ relative to that of $Sc_2S@C_2(7892)-C_{70}$.

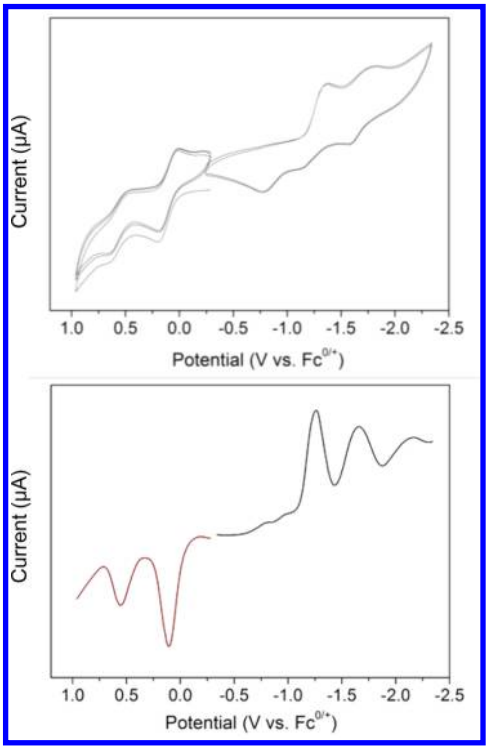

Figure 6. Cyclic voltammograms (up) and differential pulse voltammogram (down) of $Sc_2O@C_2(7892)-C_{70}$ in *o*-dichlorobenzene (0.05 M (*n*-$Bu)_4NPF_6$; scan rate 100 and 20 mV s^{-1} for CV and DPV, respectively).

4. CONCLUSIONS

In conclusion, by introducing CO_2 as the oxygen source, facile production of an extensive OCF family of $Sc_2O@C_{2n}$ (n = 35−47) has been demonstrated for the first time. Compared with the control experiments, in which the productions were performed under a pure He or He/air atmosphere, utilizing the He/CO_2 atmosphere apparently gives rise to a more selective generation of OCFs. Moreover, the $Sc_2O@C_{70}$ identified by far as the smallest OCF has been found to be available only by using the present method. The experimental and computational studies reveal that the Sc_2O can be constrained inside a small non-IPR cage of $C_2(7892)-C_{70}$, giving rise to a novel OCF with fully reversible oxidative behavior and lower bandgap relative to that of $Sc_2S@C_2(7892)-C_{70}$. To this end, these studies might open a new way to explore an extensive OCF family and underline the unique electronic and electrochemical properties of cluster fullerenes, which are internal-cluster-dependent.

■ ASSOCIATED CONTENT

Supporting Information

Detailed experimental data including HPLC profiles and mass spectra; coordination of the optimized $Sc_2O@C_2(7892)-C_{70}$ and $Sc_2S@C_2(7892)-C_{70}$; complete references. This material is available free of charge via the Internet at http://pubs.acs.org.

■ AUTHOR INFORMATION

Corresponding Authors

*E-mail: fenglai@suda.edu.cn.
*E-mail: chenning@suda.edu.cn.
*E-mail: fromzdenek@yahoo.com.
*E-mail: hailincong@yahoo.com.

Table 3. Redox Potentials (V *vs* $Fc^{0/+}$)[a] of $Sc_2O@C_2(7892)-C_{70}$ and $Sc_2S@C_2(7892)-C_{70}$

	$^{ox}E_2$	$^{ox}E_1$	$^{red}E_1$	$^{red}E_2$	$^{red}E_3$	$^{red}E_4$	EC gap
$Sc_2O@X^d$	0.55[a]	0.10[a]	−1.36[b]	−1.80[b]			1.46
$Sc_2O@X$	0.55[c]	0.10[c]	−1.25[c]	−1.66[c]	−2.15[c]		1.35
$Sc_2S@X$	0.65[b]	0.14[a]	−1.44[b]	−1.87[b]	−1.99[b]	−2.45[b]	1.58

[a]Half-wave potentials. [b]Peak potentials. [c]DPV values. [d]X = $C_2(7892)-C_{70}$

dx.doi.org/10.1021/jp509975w | J. Phys. Chem. C 2014, 118, 28883−28889

Notes

The authors declare no competing financial interest.

■ ACKNOWLEDGMENTS

This work is the supported in part by the NSFC (21241004, 51372158, 21305098, and 51302178), SRFDP (20123201120014), the NSF of Jiangsu Province (BK2012611 and BK20130295), Jiangsu Specially Appointed Professor Program (SR10800113), the Project for Jiangsu Scientific and Technological Innovation Team (2013), and the Czech Science Foundation/GACR (P208/10/1724).

■ REFERENCES

(1) Echegoyen, L.; Echegoyen, L. E. Electrochemistry of Fullerenes and Their Derivatives. *Acc. Chem. Res.* **1998**, *31*, 593−601.
(2) Guldi, D. M. Fullerenes: Three Dimensional Electron Acceptor Materials. *Chem. Commun.* **2000**, *36*, 321−327.
(3) Akasaka, T.; Nagase, S. *Endofullerenes: A New Family of Carbon Clusters*; Kluwer: Dordrecht, The Netherlands, 2002.
(4) Feng, L.; Akasaka, T.; Nagase, S. In *Carbon Nanotubes and Related Structures*; Guldi, D. M., Martin, N., Eds.; Wiley-VCH: Weinheim, Germany, 2010; p 455.
(5) Chaur, M. N.; Melin, F.; Ortiz, A. L.; Echegoyen, L. Chemical, Electrochemical, and Structural Properties of Endohedral Metallofullerenes. *Angew. Chem., Int. Ed.* **2009**, *48*, 7514−7538.
(6) Lu, X.; Feng, L.; Akasaka, T.; Nagase, S. Current Status and Future Developments of Endohedral Metallofullerenes. *Chem. Soc. Rev.* **2012**, *41*, 7723−7760.
(7) Zhang, J.; Stevenson, S.; Dorn, H. C. Trimetallic Nitride Template Endohedral Metallofullerenes: Discovery, Structural Characterization, Reactivity, and Applications. *Acc. Chem. Res.* **2013**, *46*, 1548−1557.
(8) Popov, A. A.; Yang, S.; Dunsch, L. Endohedral Fullerenes. *Chem. Rev.* **2013**, *113*, 5989−6113.
(9) Rodriguez-Fortea, A.; Balch, A. L.; Poblet, J. M. Endohedral Metallofullerenes: A Unique Host−Guest Association. *Chem. Soc. Rev.* **2011**, *40*, 3551−3563.
(10) Komatsu, K.; Murata, M.; Murata, Y. Encapsulation of Molecular Hydrogen in Fullerene C_{60} by Organic Synthesis. *Science* **2005**, *307*, 238−240.
(11) Murata, M.; Murata, Y.; Komatsu, K. Synthesis and Properties of Endohedral C_{60} Encapsulating Molecular Hydrogen. *J. Am. Chem. Soc.* **2006**, *128*, 8024−8033.
(12) Murphy, T. A.; Pawlik, T.; Weidinger, A.; Hohne, M.; Alcala, R.; Spaeth, J. M. Observation of Atomlike Nitrogen in Nitrogen-Implanted Solid C_{60}. *Phys. Rev. Lett.* **1996**, *77*, 1075−1078.
(13) Kanai, M.; Porfyrakis, K.; Briggs, G. A. D.; Dennis, T. J. S. Purification by HPLC and the UV/Vis Absorption Spectra of the Nitrogen-Containing Incar-Fullerenes iNC$_{60}$, and iNC$_{70}$. *Chem. Commun.* **2004**, 210−211.
(14) Nikawa, H.; Araki, Y.; Slanina, Z.; Tsuchiya, T.; Akasaka, T.; Wada, T.; Ito, O.; Dinse, K. P.; Ata, M.; Kato, T.; Nagase, S. The Effect of Atomic Nitrogen on the C_{60} Cage. *Chem. Commun.* **2010**, *46*, 631−633.
(15) Krause, M.; Dunsch, L. Gadolinium Nitride Gd_3N in Carbon Cages: The Influence of Cluster Size and Bond Strength. *Angew. Chem., Int. Ed.* **2005**, *44*, 1557−1560.
(16) Kurotobi, K.; Murata, Y. A. Single Molecule of Water Encapsulated in Fullerene C_{60}. *Science* **2011**, *333*, 613−616.
(17) Fatouros, P. P.; Corwin, F. D.; Chen, Z. J.; Broaddus, W. C.; Tatum, J. L.; Kettenmann, B.; Ge, Z.; Gibson, H. W.; Russ, J. L.; Leonard, A. P.; et al. In Vitro and in Vivo Imaging Studies of a New Endohedral Metallofullerene Nanoparticle. *Radiology* **2006**, *240*, 756−764.
(18) Bolskar, R. D. Gadofullerene MRI Contrast Agents. *Nanomedicine* **2008**, *3*, 201−213.
(19) Zhang, J.; Ye, Y.; Chen, Y.; Pregot, C.; Li, T.; Balasubramaniam, S.; Hobart, D. B.; Zhang, Y.; Wi, S.; Davis, R. M.; et al. Gd_3N@$C_{84}(OH)_x$: A New Egg-Shaped Metallofullerene Magnetic Resonance Imaging Contrast Agent. *J. Am. Chem. Soc.* **2014**, *136*, 2630−2636.
(20) Ross, R. B.; Cardona, C. M.; Guldi, D. M.; Sankaranarayanan, S. G.; Reese, M. O.; Kopidakis, N.; Peet, J.; Walker, B.; Bazan, G. C.; Van Keuren, E.; et al. Endohedral Fullerenes for Organic Photovoltaic Devices. *Nat. Mater.* **2009**, *8*, 208−212.
(21) Feng, L.; Rudolf, M.; Wolfrum, S.; Troeger, A.; Slanina, Z.; Akasaka, T.; Nagase, S.; Martin, N.; Ameri, T.; Brabec, C. J.; et al. A Paradigmatic Change: Linking Fullerenes to Electron Acceptors. *J. Am. Chem. Soc.* **2012**, *134*, 12190−12197.
(22) Rudolf, M.; Feng, L.; Slanina, Z.; Akasaka, T.; Nagase, S.; Guldi, D. M. A Metallofullerene Electron Donor that Powers an Efficient Spin Flip in a Linear Electron Donor-Acceptor Conjugate. *J. Am. Chem. Soc.* **2013**, *135*, 11165−11174.
(23) Liang, Y.; Feng, L. Dual Electron Acceptor/Electron Donor Character of Endohedral Nitride Clusterfullerenes. *Fullerenes, Nanotubes, Carbon Nanostruct.* **2014**, *22*, 227−234.
(24) Nishibori, E.; Takata, M.; Sakata, M.; Tanaka, H.; Hasegawa, M.; Shinohara, H. Giant Motion of La Atom inside C_{82} Cage. *Chem. Phys. Lett.* **2000**, *330*, 497−502.
(25) Akasaka, T.; Nagase, S.; Kobayashi, K.; Walchli, M.; Yamamoto, K.; Funasaka, H.; Kako, M.; Hoshino, T.; Erata, T. ^{13}C and ^{139}La NMR Studies of La_2@C_{80}: First Evidence for Circular Motion of Metal Atoms in Endohedral Dimetallofullerenes. *Angew. Chem., Int. Ed.* **1997**, *36*, 1643−1645.
(26) Popov, A. A.; Zhang, L.; Dunsch, L. A. Pseudoatom in a Cage: Trimetallofullerene Y_3@C_{80} Mimics Y_3N@C_{80} with Nitrogen Substituted by a Pseudoatom. *ACS Nano* **2010**, *4*, 795−802.
(27) Xu, W.; Feng, L.; Calvaresi, M.; Liu, J.; Liu, Y.; Niu, B.; Shi, Z.; Lian, Y.; Zerbetto, F. An Experimentally Observed Trimetallofullerene Sm_3@I_h-C_{80}: Encapsulation of Three Metal Atoms in a Cage without a Nonmetallic Mediator. *J. Am. Chem. Soc.* **2013**, *135*, 4187−4190.
(28) Wang, C. R.; Tan, K.; Tomiyama, T.; Yoshida, T.; Kobayashi, Y.; Nishibori, E.; Takata, M.; Sakata, M.; Shinohara, H. A. Scandium Carbide Endohedral Metallofullerene: (Sc_2C_2)@C_{80}. *Angew. Chem., Int. Ed.* **2001**, *40*, 397−399.
(29) Iiduka, Y.; Wakahara, T.; Nakahodo, T.; Tsuchiya, T.; Sakuraba, A.; Maeda, Y.; Akasaka, T.; Yoza, K.; Horn, E.; Kato, T.; et al. Structural Determination of Metallofullerene Sc_3C_{82} Revisited: A Surprising Finding. *J. Am. Chem. Soc.* **2005**, *127*, 12500−12501.
(30) Kurihara, H.; Lu, X.; Iiduka, Y.; Mizorogi, N.; Slanina, Z.; Tsuchiya, T.; Akasaka, T.; Nagase, S. Sc_2C_2@C_{80} Rather than Sc_2@C_{82}: Templated Formation of Unexpected $C_{2v}(5)$-C_{80} and Temperature-Dependent Dynamic Motion of Internal Sc_2C_2 Cluster. *J. Am. Chem. Soc.* **2011**, *133*, 2382−2385.
(31) Lu, X.; Nakajima, K.; Iiduka, Y.; Nikawa, H.; Mizorogi, N.; Slanina, Z.; Tsuchiya, T.; Nagase, S.; Akasaka, T. Structural Elucidation and Regioselective Functionalization of An Unexplored Carbide Cluster Metallofullerene Sc_2C_2@$C_s(6)$-C_{82}. *J. Am. Chem. Soc.* **2011**, *133*, 19553−19558.
(32) Lu, X.; Nakajima, K.; Iiduka, Y.; Nikawa, H.; Tsuchiya, T.; Mizorogi, N.; Slanina, Z.; Nagase, S.; Akasaka, T. The Long-Believed Sc_2@$C_{2v}(17)$-C_{84} is Actually Sc_2C_2@$C_{2v}(9)$-C_{82}: Unambiguous Structure Assignment and Chemical Functionalization. *Angew. Chem., Int. Ed.* **2012**, *51*, 5889−5892.
(33) Stevenson, S.; Rice, G.; Glass, T.; Harich, K.; Cromer, F.; Jordan, M. R.; Craft, J.; Hadju, E.; Bible, R.; Olmstead, M. M.; et al. Small-Bandgap Endohedral Metallofullerenes in High Yield and Purity. *Nature* **1999**, *401*, 55−57.
(34) Zuo, T. M.; Beavers, C. M.; Duchamp, J. C.; Campbell, A.; Dorn, H. C.; Olmstead, M. M.; Balch, A. L. Isolation and Structural Characterization of a Family of Endohedral Fullerenes Including the Large, Chiral Cage Fullerenes Tb_3N@C_{88} and Tb_3N@C_{86} as well as the I_h and D_{5h} Isomers of Tb_3N@C_{80}. *J. Am. Chem. Soc.* **2007**, *129*, 2035−2043.
(35) Beavers, C. M.; Chaur, M. N.; Olmstead, M. M.; Echegoyen, L.; Balch, A. L. Large Metal Ions in a Relatively Small Fullerene Cage: The Structure of Gd_3N@$C_2(22010)$-C_{78} Departs from the Isolated Pentagon Rule. *J. Am. Chem. Soc.* **2009**, *131*, 11519−11524.

(36) Dunsch, L.; Yang, S.; Zhang, L.; Svitova, A.; Oswald, S.; Popov, A. A. Metal Sulfide in a C_{82} Fullerene Cage: A New Form of Endohedral Clusterfullerenes. *J. Am. Chem. Soc.* **2010**, *132*, 5413−5421.
(37) Chen, N.; Chaur, M. N.; Moore, C.; Pinzon, J. R.; Valencia, R.; Rodriguez-Fortea, A.; Poblet, J. M.; Echegoyen, L. Synthesis of a New Endohedral Fullerene Family, $Sc_2S@C_{2n}$ (n = 40−50) by the Introduction of SO_2. *Chem. Commun.* **2010**, *46*, 4818−4820.
(38) Mercado, B. Q.; Chen, N.; Rodríguez-Fortea, A.; Mackey, M. A.; Stevenson, S.; Echegoyen, L.; Poblet, J. M.; Olmstead, M. M.; Balch, A. L. The Shape of the $Sc_2(\mu_2\text{-}S)$ Unit Trapped in C_{82}: Crystallographic, Computational, and Electrochemical Studies of the Isomers, $Sc_2(\mu_2\text{-}S)@C_s(6)\text{-}C_{82}$ and $Sc_2(\mu_2\text{-}S)@C_{3v}(8)\text{-}C_{82}$. *J. Am. Chem. Soc.* **2011**, *133*, 6752−6760.
(39) Wang, T. S.; Feng, L.; Wu, J. Y.; Xu, W.; Xiang, J. F.; Tan, K.; Ma, Y. H.; Zheng, J. P.; Jiang, L.; Lu, X.; et al. Planar Quinary Cluster inside a Fullerene Cage: Synthesis and Structural Characterizations of $Sc_3NC@C_{80}\text{-}I_h$. *J. Am. Chem. Soc.* **2010**, *132*, 16362−16364.
(40) Yang, S. F.; Chen, C. B.; Liu, F. P.; Xie, Y. P.; Li, F. Y.; Jiao, M. Z.; Suzuki, M.; Lu, X.; Akasaka, T.; et al. An Improbable Monometallic Cluster Entrapped in a Popular Fullerene Cage: $YCN@C_s(6)\text{-}C_{82}$. *Sci. Rep.* **2013**, *3*, 1487−1491.
(41) Liu, F.; Wang, S.; Guan, J.; Wei, T.; Zeng, M.; Yang, S. Putting a Terbium-Monometallic Cyanide Cluster into the C_{82} Fullerene Cage: $TbCN@C_2(5)\text{-}C_{82}$. *Inorg. Chem.* **2014**, *53*, 5201−5205.
(42) Stevenson, S.; Mackey, M. A.; Stuart, M. A.; Phillips, J. P.; Easterling, M. L.; Chancellor, C. J.; Olmstead, M. M.; Balch, A. L. A Distorted Tetrahedral Metal Oxide Cluster inside an Icosahedral Carbon Cage. Synthesis, Isolation, and Structural Characterization of $Sc_4(\mu_3\text{-}O)_2@I_h\text{-}C_{80}$. *J. Am. Chem. Soc.* **2008**, *130*, 11844−11845.
(43) Mercado, B. Q.; Stuart, M. A.; Mackey, M. A.; Pickens, J. E.; Confait, S. B.; Stevenson, S.; Easterling, M. L.; Valencia, R.; Rodríguez-Fortea, A.; Poblet, J. M.; et al. $Sc_2(\mu_2\text{-}O)$ Trapped in a Fullerene Cage: The Isolation and Structural Characterization of $Sc_2(\mu_2\text{-}O)@C_s(6)\text{-}C_{82}$ and the Relevance of the Thermal and Entropic Effects in Fullerene Isomer Selection. *J. Am. Chem. Soc.* **2010**, *132*, 12098−12105.
(44) Mercado, B. Q.; Olmstead, M. M.; Beavers, C. M.; Easterling, M. L.; Stevenson, S.; Mackey, M. A.; Coumbe, C. E.; Phillips, J. D.; Phillips, J. P.; Poblet, J. M.; et al. A Seven Atom Cluster in a Carbon Cage, the Crystallographically Determined Structure of $Sc_4(\mu_3\text{-}O)_3@I_h\text{-}C_{80}$. *Chem. Commun.* **2010**, *46*, 279−281.
(45) Krätschmer, W.; Lamb, L. D.; Fostiropoulos, K.; Huffman, D. R. Solid C_{60}: a New Form of Carbon. *Nature* **1990**, *347*, 354−358.
(46) Yang, S.; Kalbac, M.; Popov, A. A.; Dunsch, L. A Facile Route to the Non-IPR Fullerene $Sc_3N@C_{68}$: Synthesis, Spectroscopic Characterization, and Density Functional Theory Computations (IPR=Isolated Pentagon Rule). *Chem.—Eur. J.* **2006**, *12*, 7856−7863.
(47) Yang, S.; Popov, A. A.; Dunsch, L. Violating the Isolated Pentagon Rule (IPR): the Endohedral Non-IPR C_{70} Cage of $Sc_3N@C_{70}$. *Angew. Chem., Int. Ed.* **2007**, *46*, 1256−1259.
(48) Chen, N.; Mulet-Gas, M.; Li, Y.; Stene, R. E.; Atherton, C. W.; Rodríguez-Fortea, A.; Poblet, J. M.; Echegoyen, L. $Sc_2S@C_2(7892)\text{-}C_{70}$: a Metallic Sulfide Cluster inside a Non-IPR C_{70} Cage. *Chem. Sci.* **2013**, *4*, 180−186.
(49) Shinohara, H. Endohedral Metallofullerenes. *Rep. Prog. Phys.* **2000**, *63*, 843.
(50) Zhao, Y.; Truhlar, D. G. The M06 Suite of Density Functionals for Main Group Thermochemistry, Thermochemical Kinetics, Noncovalent Interactions, Excited States, and Transition Elements: Two New Functionals and Systematic Testing of Four M06-class Functionals and 12 Other Functional. *Theor. Chem. Acc.* **2008**, *120*, 215−241.
(51) Becke, A. D. Density-functional Thermochemistry. III. The Role of Exact Exchange. *J. Chem. Phys.* **1993**, *98*, 5648−5652.
(52) Cao, X.; Dolg, M. Optimized Basis Sets for Lanthanide and Actinide Systems and Their Application in Quantum Chemical Calculations. *Theochem* **2002**, *581*, 139−147.
(53) Electronegativity using the Allen scale. Allen, L. C. Electronegativity is the Average One-electron Energy of the Valence-shell Electrons in Ground-state Free Atoms. *J. Am. Chem. Soc.* **1989**, *111*, 9003−9014.
(54) Stevenson, S.; Fowler, P. W.; Heine, T.; Duchamp, J. C.; Rice, G.; Glass, T.; Harich, K.; Hajdu, E.; Bible, R.; Dorn, H. C. Materials Science: A Stable Non-classical Metallofullerene Family. *Nature* **2000**, *408*, 427−428.
(55) Mercado, B. Q.; Beavers, C. M.; Olmstead, M. M.; Chaur, M. N.; Walker, K.; Holloway, B. C.; Echegoyen, L.; Balch, A. L. Is the Isolated Pentagon Rule Merely a Suggestion for Endohedral Fullerenes? The Structure of a Second Egg-Shaped Endohedral Fullerene-$Gd_3N@C_s(39663)\text{-}C_{82}$. *J. Am. Chem. Soc.* **2008**, *130*, 7854−7855.
(56) Chen, N.; Beavers, C. M.; Mulet-Gas, M.; Rodríguez-Fortea, A.; Munoz, E. J.; Li, Y.-Y.; Olmstead, M. M.; Balch, A. L.; Poblet, J. M.; Echegoyen, L. $Sc_2S@C_s(10528)\text{-}C_{72}$: a Dimetallic Sulfide Endohedral Fullerene with a Non Isolated Pentagon Rule Cage. *J. Am. Chem. Soc.* **2012**, *134*, 7851−7860.